Acta Biomaterialia 6 (2010) 1219–1226

Contents lists available at ScienceDirect

Acta Biomaterialia

journal homepage: www.elsevier.com/locate/actabiomat

Biodegradable fibrous scaffolds with diverse properties by electrospinning candidates from a combinatorial macromer library

Robert B. Metter [a], Jamie L. Ifkovits [a], Kevin Hou [a], Ludovic Vincent [a], Benjamin Hsu [a], Louis Wang [a], Robert L. Mauck [b], Jason A. Burdick [a,*]

[a] Department of Bioengineering, University of Pennsylvania, 240 Skirkanich Hall, 210 S. 33rd Street, Philadelphia, PA 19104, USA
[b] Mckay Orthopaedic Research Laboratory, Department of Orthopaedic Surgery, University of Pennsylvania, Philadelphia, PA 19104, USA

ARTICLE INFO

Article history:
Received 18 August 2009
Received in revised form 2 October 2009
Accepted 15 October 2009
Available online 21 October 2009

Keywords:
Electrospinning
Macromer
Biodegradable
Polymer
Tissue engineering

ABSTRACT

The properties of electrospun fibrous scaffolds, including degradation, mechanics and cellular interactions, are important for their use in tissue engineering applications. Although some diversity has been obtained previously in fibrous scaffolds, optimization of scaffold properties relies on iterative techniques in both polymer synthesis and processing. Here, we electrospun candidates from a combinatorial library of biodegradable and photopolymerizable poly(β-amino ester)s (PBAEs) to show that the diversity in properties found in this library is retained when processed into fibrous scaffolds. Specifically, three PBAE macromers were electrospun into scaffolds and possessed similar initial mechanical properties, but exhibited mass loss ranging from rapid (complete degradation within ~2 weeks) to moderate (complete degradation within ~3 months) to slow (only partial degradation after 3 months). These trends in mechanics and degradation mimicked what was previously observed in the bulk polymers. Although cellular adhesion was dependent on the polymer composition in films, adhesion to scaffolds that were electrospun with gelatin was similar on all formulations and controls. To further illustrate the diverse properties that are attainable in these systems, the fastest and slowest degrading polymers were electrospun together into one scaffold, but as distinct fiber populations. This dual-polymer scaffold exhibited behavior in mass loss and mechanics with time that fell between the single-polymer scaffolds. In general, this work indicates that combinatorial libraries may be an important source of information and specific polymer compositions for the fabrication of electrospun fibrous scaffolds with tunable properties.

1. Introduction

Electrospun fibrous scaffolds are finding widespread application in numerous tissue engineering approaches, particularly for fiber-reinforced tissues, such as myocardium, the annulus fibrosis of the intervertebral disc, meniscus, tendons, and ligaments [1]. The benefits of such fibrous scaffolds have been reviewed extensively elsewhere [2–4] and include a size-scale similar to the native extracellular matrix and the ability to promote alignment of cells and anisotropy in developing tissues through fiber alignment. It is becoming apparent that the physical and chemical properties of the scaffold are crucial in their success towards the engineering of tissues and in controlling cellular behavior. Scaffolds must exhibit mechanical properties that are sufficient for stability during tissue development and in the site of implantation, and must degrade at an appropriate rate to support, yet not inhibit, matrix production and development. From a cellular perspective, a range of cues such as the material properties and their presentation in time and space are important [5], in addition to diffusivity and potential toxicity of degradation products.

A range of both synthetic [6–8] and natural [9–12] polymers have been successfully electrospun into fibrous scaffolds; however, the ability to modify the scaffold properties with these polymer formulations is limited and involves iteration of synthesis and processing steps. Also, many properties (e.g. mechanics and degradation) in polymers are directly coupled, further limiting the scaffold properties that are possible. One approach that has increased the diversity of polymer properties available for scaffold fabrication is the use of combinatorial polymer libraries [13–15]. The development of combinatorial libraries uses concepts that have been utilized in drug development for many years, namely rapid and parallel synthetic techniques to synthesize a large number of molecules [16]. Thus, these polymer libraries may allow for similar diversity in scaffolding for tissue engineering.

Examples of combinatorial libraries of polymers include polyarylates [17,18] and poly(β-amino ester)s (PBAEs) [19–21]. PBAEs are synthesized through the addition reaction of commercially available amines and diacrylates without any byproducts that need purification, which accelerates their synthesis [21]. This class of

* Corresponding author. Tel.: +1 215 898 8537; fax: +1 215 573 2071.
E-mail address: burdick2@seas.upenn.edu (J.A. Burdick).

1742-7061/$ - see front matter © 2009 Acta Materialia Inc. Published by Elsevier Ltd. All rights reserved.
doi:10.1016/j.actbio.2009.10.027

materials was originally developed for gene therapy, but recent work includes their use in the development of tissue engineering scaffolds [22]. To accomplish this, PBAE macromers were synthesized with acrylate end groups (molar ratio of diacrylate to amine >1) that can be crosslinked into networks with the addition of light and a photoinitiator [22]. Network degradation times ranged from less than 1 day to over 4 months and the mechanics spanned two orders of magnitude (from ~2 to ~200 MPa). The library was further expanded by investigating the influence of macromer molecular weight (through changes in the ratio of acrylate to amine) and macromer branching (through introduction of a triacrylate) on network properties [23,24]. This led to changes in network mechanical properties, degradation rates and cell adhesion. Importantly, the mechanical properties of networks formed from this macromer library appear to be decoupled from mass loss, so combinations of properties are not limited.

Only recently has electrospinning been performed with low molecular weight and radically polymerizable macromers. Tan et al. [25] showed that macromers could be electrospun in the presence of a photoinitiator and a carrier polymer (to facilitate fiber formation) and subsequently crosslinked with light exposure. These macromers reached high reactive group conversion in the fiber form, formed uniform fibers and could be processed either as a random sheet or aligned by spinning on a mandrel [25]. The primary objective of the work presented here was to electrospin select candidate macromers from this PBAE combinatorial library to obtain scaffolds with diverse properties that correlated to those found in their original assessment. Additionally, this diversity is exploited by using a recently developed multi-polymer electrospinning system [26,27] to further introduce complexity into these scaffolds through combinations of distinct polymer populations. The novelty of this work is that properties that range orders of magnitude and are decoupled from each other can be obtained from a combinatorial system that cannot be found with distinct polymers. This work will hopefully provide platform technology for a range of tissue engineering systems that require controllable scaffold properties.

2. Materials and methods

2.1. Macromer synthesis and characterization

Acrylate-terminated PBAEs were synthesized by the step-growth polymerization of a commercially available primary amine, isobutylamine (6, Sigma), with one of three different diacrylates, poly(ethylene glycol)-200 diacrylate (D, Scientific Polymer Products, Inc.), diethylene glycol diacrylate (A, Scientific Polymer Products, Inc.) and 1,4-butanediol diacrylate (B, Scientific Polymer Products, Inc.). The sample notation is consistent with our previous report on the development of the initial PBAE library [22]. These liquid reagents were mixed at a molar ratio of diacrylate to amines of either 1.2 (A6, B6) or 1.35 (D6) in glass scintillation vials at 90 °C overnight while stirring (700 rpm, Telesystem HP15/RM, Variomag, USA). The molecular weights of D6, A6 and B6 macromers were determined using ^{1}H NMR (Bruker Advance 360 MHz, Bruker, Billerica, MA) as in Ref. [23].

2.2. Electrospinning single and dual-polymer scaffolds

Polymers were electrospun using a custom dual-jet electrospinning apparatus [26]. The electrospinning solutions consisted of 8.75 wt.% of the PBAE macromer (D6, A6 or B6), 3.25 wt.% gelatin B (Sigma) and 0.45 wt.% photoinitiator (2-dimethoxy-2-phenyl acetophenone, DMPA, Sigma) in 1,1,1,3,3,3-hexafluoroisopropanol (HFIP, Sigma), for a mass ratio of 73:27 PBAE:gelatin. Spinning solutions were loaded into 20 ml plastic syringes fitted with 5 cm lengths of flexible silicon tubing connected to an 18 gauge blunt 6" stainless steel needle. The needles cycled along a 7 cm path length along the mandrel via two custom-built fanners. For aligned samples, fibers were collected on a rotating mandrel (2" diameter, 8" length) spinning at a linear velocity of 10 m s^{-1}. After optimization (via fiber integrity with scanning electron microscopy, SEM), A6 was spun at a tip to mandrel distance of 10 cm, while B6 and D6 were spun at 8 cm. For all three polymers, a voltage bias of +20 kV was maintained between the spinneret and the grounded mandrel by a power supply (ES30N-5W, Gamma High Voltage Research, Inc., Ormand Beach, FL), and a flow rate of 1.5 ml h^{-1} was controlled via a syringe pump (KDS100, KD Scientific, Holliston, MA). Polymers were electrospun for 12 h to obtain full-thickness scaffolds. Both single- (D6, A6, B6) and dual-polymer (D6/B6) scaffolds were fabricated using two jets on the dual-jet system, either with the same solution in each syringe for the uniform scaffolds or different solutions for the dual-polymer ones.

The formation of two distinct sets of fibers in the composite scaffold was confirmed by visualization using a fluorescent dye in one fiber population and comparing to a light micrographic image of the fiber mixture. Specifically, the B6 electrospinning solution was doped with methacryloxethyl thiocarbamoyl rhodamine B (100 μM, Polysciences, Warrington, PA), whereas the D6 solution did not contain a dye. The composite scaffold was electrospun onto glass coverslips affixed to the mandrel using the previously described conditions for 30 s. Samples were removed and imaged using a fluorescent microscope (Axiovert, Zeiss, Germany) with a digital camera (Axiovision, Zeiss).

2.3. Polymerization

For slab formation, DMPA was dissolved in HFIP and added directly to the liquid macromer for a final concentration of 0.5 wt.% initiator. HFIP was evaporated from the mixture and the macromer/initiator solution was placed between glass slides with a 1 mm spacer and exposed to ultraviolet light (10 mW cm^{-2}, Black-Ray) for 10 min. For mechanical and degradation studies, rectangular samples (5 × 25 mm) were cut from the slabs.

For fibrous scaffolds, the electrospun macromer mats (containing photoinitiator) were removed from the mandrel, placed in a nitrogen chamber (to prevent oxygen inhibition of polymerization at fiber surfaces) and exposed to ultraviolet light (10 mW cm^{-2}, Black-Ray) for 10 min. Rectangular samples (5 × 25 mm) were cut from the crosslinked fibrous mats for mechanical and degradation studies.

2.4. Fiber characterization

Scaffolds were visualized by SEM (JEOL 7500F HRSEM, Penn Regional Nanotechnology Facility) after crosslinking. Fiber diameters were quantified using the length measurement tool in ImageJ (v1.42q, NIH). One hundred measurements were taken for each SEM image for each scaffold in both non-aligned and aligned structures. The fiber alignment was also quantified using ImageJ, by measuring the angle of each fiber (>120 per scaffold) with respect to a reference angle.

Uniaxial tensile testing (n = 3) was performed on both slabs and fibrous samples (non-aligned and aligned) using an Instron 5848 Microtester with serrated vice grips and a 50 N load cell (Instron, Canton, MA). The cross-sectional area was determined by either measuring samples with a digital caliper (slabs) or using a custom laser measurement system (fibrous scaffolds, five measurements along the width of each sample). Slabs were tested by extending the samples at a failure rate of 0.1% of the gauge length per second, as in Ref. [28]. Fibrous scaffolds were tested by preconditioning

with 10 cycles of extension to 0.5% of the gauge length at a frequency of 0.1 Hz and then extending the sample to failure at a rate of 0.1% of the gauge length per second. The moduli were calculated from the linear region of the stress–strain curve and initial sample geometry.

Degradation ($n = 3$) of slabs and fibrous samples (aligned) was performed by incubating the samples in phosphate-buffered saline at 37 °C for up to 12 weeks. At each time point, the samples were tested for mechanical properties as above, lyophilized and weighed to obtain the final sample mass. The mass loss was determined as the difference between the final and the initial mass divided by the initial mass.

2.5. Cellular interactions

To prepare films for cell interaction studies, the macromer/initiator solutions were dissolved in ethanol at 50 wt.% and pipetted (35 μl) into 24-well plates. The ethanol was allowed to evaporate off overnight to leave a thin film of the macromer and initiator. The plates were placed in a nitrogen chamber and polymerized as above. To investigate cellular interactions with fibrous scaffolds, macromer solutions were electrospun directly onto methacrylated coverslips for 40 min, crosslinked as above and placed in 6-well plates. For both groups, plates containing the samples were placed under a germicidal lamp in a laminar flow hood for 1 h, incubated in sterile PBS overnight and incubated with growth medium (alpha-MEM (Gibco, Invitrogen, Carlsbad, CA) supplemented with 16.7% fetal bovine serum (Gibco), 1% penicillin (Gibco) and 1% streptomycin (Gibco)) for 1 h prior to cell seeding.

Human mesenchymal stem cells (hMSCs, Lonza) were maintained in standard growth medium and seeded (6000 cells cm^{-2}) onto the films and scaffolds. Cell viability/proliferation ($n = 3$) was measured using the AlamarBlue™ (AB, Invitrogen) fluorescence assay. Briefly, growth medium containing 10 vol.% AB was added to each well at each time point (1, 4 and 7 days). After a 5 h incubation period, 100 μl aliquots ($n = 3$ per group) of the AB containing medium were removed from each well for fluorescence measurement (530 nm excitation, 590 nm emission, Synergy HT, Biotek Winooski, VT). Cells were then fed with fresh growth medium without AB. After 1 week, the cells were fixed in 10% formalin and stained for actin organization with fluorescein isothiocyanate-conjugated phalloidin (1 μg ml^{-1} in blocking solution, Sigma) for 40 min at room temperature and nuclei with 4′,6-diamidino-2-phenylindole (1:2500, Sigma) for 5 min at room temperature. Samples were visualized on a fluorescent microscope (Axiovert, Zeiss) with a digital camera (Axiovision, Zeiss).

2.6. Statistical analysis

Statistical analysis was performed using analysis of variance with Tukey's post hoc test among the groups, with significance defined as a confidence level of 0.05. All values are reported as the mean and standard deviation of the mean.

3. Results and discussion

Three macromers (D6, A6 and B6) that exhibited diverse properties in a previous investigation of a combinatorial library of photopolymerizable and degradable macromers were synthesized and used to illustrate the diversity that is attainable in electrospun scaffolds from this library. These acrylate-terminated and degradable macromers (Fig. 1) were synthesized using an addition reaction with the same primary amine component (isobutylamine), but with variable diacrylates (poly(ethylene glycol)-200 diacrylate, diethylene glycol diacrylate or 1,4-butanediol diacrylate). The

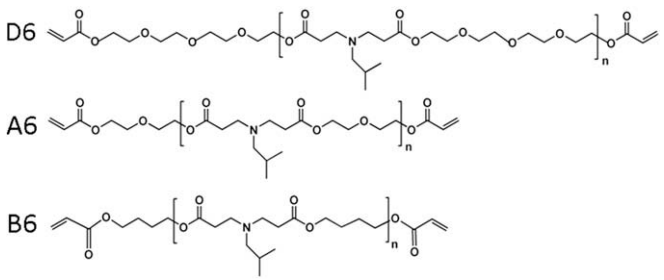

Fig. 1. Chemical structures of D6, A6 and B6 macromers. The macromers are synthesized by the reaction of isobutylamine (6) with poly(ethylene glycol)-200 diacrylate (D), diethylene glycol diacrylate (A) or 1,4-butanediol diacrylate (B) to obtain acrylate-terminated macromers that form crosslinked networks in the presence of light and a photoinitiator.

acrylate-terminated macromers all had a molecular weight in the range of ~1.9 to 3.0 kDa and could be crosslinked into networks using a free-radical photoinitiated polymerization. There is chemical similarity between the macromers, particularly since the same amine was used during synthesis, but the backbone varies with respect to the number of ethylene glycol repeat units or aliphatic chain length. Water contact angles were assessed on films of each of these polymer networks and determined to be 16.2 ± 5.6, 35.5 ± 7.9 and 66.7 ± 3.1 for D6, A6 and B6, respectively. This indicates that the networks are varied in their hydrophobicity and that D6 is the most hydrophilic, whereas B6 is the most hydrophobic. This is not unexpected since D6 has the greatest number of hydrophilic ethylene glycol units in the backbone, whereas B6 includes more hydrophobic carbon–carbon bonds.

Using a recently developed process [25,29], the macromers and a photoinitiator were electrospun into individual fibrous scaffolds with gelatin as a carrier polymer to facilitate fiber formation. Previous work [25,29] indicated that the low molecular weight macromers are not able to form fibers alone, potentially due to limited polymer entanglement with these short lengths. However, a carrier polymer (i.e. gelatin) of a higher molecular weight is able to undergo electrospinning and "carry" the macromer with it into the fiber. The amount of gelatin necessary and the electrospinning parameters were determined in pilot studies to optimize fiber morphology while maximizing the amount of the PBAE polymer, to retain the polymer properties in the scaffold rather than those of the gelatin. With this in mind, 73% polymer and 27% gelatin by weight in the resulting scaffold met this criterion and uniform fibers were produced that could be crosslinked with light exposure at high conversions (>95%) of reactive groups. It is expected that the fibers are crosslinked both within and between fibers, leading to stable fibrous scaffolds.

SEM images of the fibers electrospun either onto a horizontal plate (non-aligned) or onto a rotating mandrel (aligned) are shown in Fig. 2A. All fibers were ~250–400 nm in diameter and there were no statistically significant differences between fiber sizes regardless of the polymer chemistry or fiber alignment, except for the aligned B6 formulation. Specifically, the D6, A6 and B6 were 300 ± 106, 375 ± 232 and 399 ± 213 mm in diameter, respectively, in the non-aligned scaffolds and 249 ± 102, 258 ± 78 and 703 ± 286 mm in diameter, respectively, in the aligned scaffolds. Nearly identical electrospinning parameters were used for the production of all scaffolds since the chemistry varies only moderately between groups and the molecular weights are similar. The discrepancy with the B6 formulation could be due to non-optimized parameters for electrospinning, as more welding of fibers in the aligned direction is observed in the SEM images. However, alignment of the fibers was possible with the mandrel, as evident by a low fiber angle (~20°, results not shown) that was observed in

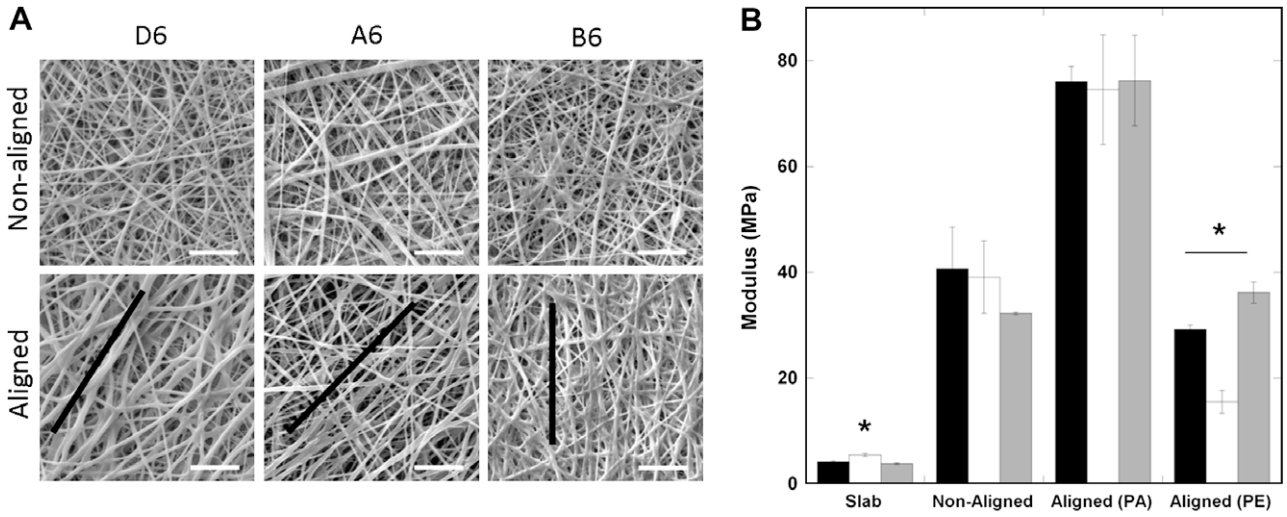

Fig. 2. Fiber structure and initial scaffold mechanics. (A) SEM images of both aligned and non-aligned D6, A6 and B6 fibrous scaffolds after electrospinning and crosslinking (scale bar = 5 μm). The general direction of alignment is denoted by the black line. (B) Initial tensile modulus of the D6 (black), A6 (white) and B6 (grey) polymers assessed as slabs and both non-aligned and aligned fibrous scaffolds, tested in both the parallel (PA) and perpendicular (PE) directions. * Statistically significant difference ($p < 0.05$) between that polymer and other polymers tested in the same format (e.g. slab).

the direction of alignment for samples that were electrospun onto a rotating mandrel.

Tensile testing was performed on PBAE polymer slabs, as well as fibrous scaffolds for both non-aligned and aligned structures. In general, there were no major differences between the groups (Fig. 2B), regardless of structure, although there were some exceptions. A6 was slightly higher in the slab form and lower in the aligned fibrous scaffolds tested in the direction perpendicular to alignment. This may be because of the lower fiber welding, due to more distinct fibers, which decreases the surface area that is shared between fibers. Regardless, the stress–strain profiles were relatively linear throughout the testing for all polymer formulations in both the slab and fibrous scaffold forms. The polymer slabs exhibited a modulus of ~5 MPa, whereas the moduli for non-aligned scaffolds were ~35–40 MPa. Although the scaffolds are much more porous than the slabs, it is not unexpected that they have higher moduli due to the gelatin content. Electrospun dry gelatin scaffolds alone have a modulus of ~500 MPa [30], which is much greater than these crosslinked slab materials. As an indication of the anisotropy of the aligned scaffolds, the moduli increased nearly two-fold when the scaffolds were tested in the aligned direction. An anisotropy ratio ranging from 2 to 5 is observed for the scaffolds when tested in the direction parallel compared to perpendicular to the orientation of the fibers. Although these three candidate polymers have similar mechanics, they were chosen based on their diversity in degradation. Additional candidates from the original polymer library [19] could be selected based on mechanical diversity to alter these properties since they ranged over two orders of magnitude.

The mass loss profiles for the selected polymers as both slabs and aligned fibrous scaffolds are shown in Fig. 3. For slabs, the D6 networks degrade entirely with 2 weeks of incubation in a buffered solution, whereas the A6 networks remain until 12 weeks, and the B6 networks have only lost ~45% of their mass at the 12 week time point (Fig. 3A). Although the polymers were identified by their previously assessed degradation in the combinatorial library study, the objective of that work was random combinations of polymer components rather than trying to elucidate different mechanisms for the performance of specific polymers. Here, the contact angle measurements can help to explain the mass loss profiles. Since D6 is the most hydrophilic, water uptake may be much more rapid and available for cleavage of degradable esters, whereas water may be limited for degradation of the more hydrophobic B6 networks. In these slowly degrading B6 networks, mass loss is minimal after an initial burst (~5%) and then the rate of mass loss increases (increasing slope) with time.

These same mass loss trends are also observed in the fibrous scaffolds (Fig. 3B), illustrating the diversity that is possible with candidates from the PBAE combinatorial library. The D6 scaffolds are again completely degraded within 2 weeks, the A6 scaffolds are nearly degraded by 12 weeks and the B6 scaffolds have lost ~50% of their mass by 12 weeks. However, the mass loss profiles are slightly different for the scaffolds. Here, the initial rate of mass loss is quite fast and then decreases. This initial mass loss may be attributed to gelatin being released from the networks. Gelatin is not crosslinked into the network, but is supported as a semi-interpenetrating network within the PBAE crosslinked networks and may diffuse out. Also, the presence of gelatin may alter the PBAE structure, which could change how mass is lost throughout. Unfortunately, it was not possible to incorporate gelatin into the bulk slabs, due to phase separation and the need for solvent removal, so it is only possible to comment on the potential influence of gelatin. Importantly, the general trends of mass loss in the bulk slabs are preserved in the scaffolds.

The moduli of slabs (Fig. 4A) and scaffolds (Fig. 4B) were also measured with degradation. The modulus of both types of structures decreased with degradation as crosslinks are broken in the networks, leading to a decrease in the crosslinking density. The rate at which the modulus decreased correlated to the timing of the scaffold degradation in both slabs and scaffolds. For the scaffolds, a rapid decrease in modulus was observed with hydration and swelling of the gelatin, whereas the properties were similar before and after hydration for the slabs. Thus, in many cases the hydrated scaffolds have mechanical properties lower than the slabs, even though the scaffolds were much greater than the slabs in the dry state. It is important to understand how the mechanical properties change with time, when targeting specific applications, and the diversity that is again possible in this behavior.

As a representative anchorage-dependent cell, MSCs were seeded onto the surfaces of films and scaffolds of D6, A6 and B6 polymers. When seeded onto the polymer films, the cellular activity (measured with the Alamar Blue assay) was highly dependent

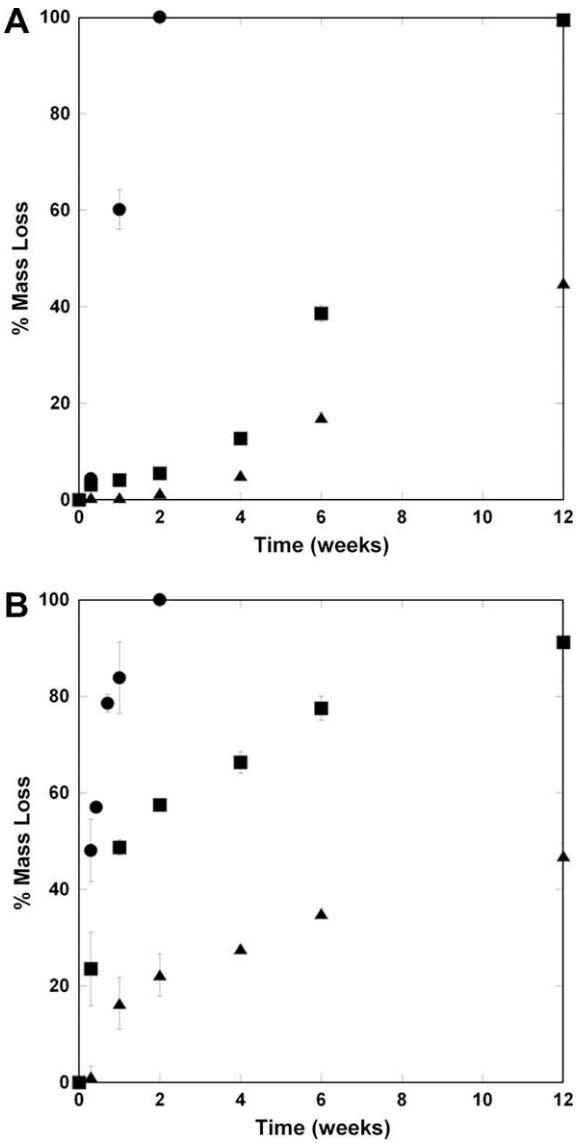

Fig. 3. Degradation behavior. (A) Mass loss profiles for slabs of D6 (circles), A6 (squares) and B6 (triangles) polymers. (B) Mass loss profiles for aligned fibrous scaffolds of D6 (circles), A6 (squares) and B6 (triangles) polymers.

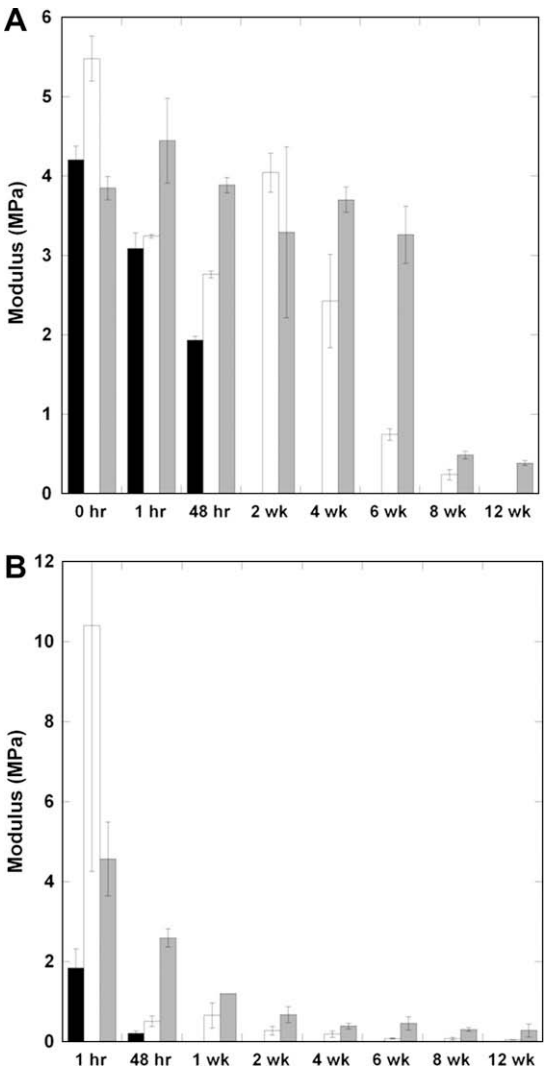

Fig. 4. Mechanics with degradation. (A) Tensile modulus of slabs of D6 (black), A6 (white) and B6 (grey) polymers with degradation. (B) Tensile modulus of slabs of aligned fibrous scaffolds of D6 (black), A6 (white) and B6 (grey) polymers with degradation. The D6 scaffolds were not testable after the 48 h time point.

on the polymer chemistry (Fig. 5A). A trend of enhanced cell numbers was observed with increased polymer hydrophobicity (B6 > A6 > D6) and few cells remained on the D6 networks after 1 day. This is likely due to differences in protein adsorption on the surfaces, which mediates adhesion on the polymers, and potential toxicity of degradation products since they are released so quickly. It is known that protein adsorption is greater on hydrophobic polymer surfaces and minimal on hydrophilic polymers [31,32]. MSC numbers increased with culture on the A6 and B6 polymers, but were inferior to the control system after 7 days. This may be due to non-optimized initial cellular adhesion on the polymers. However, this same trend was not observed with respect to MSC interactions with the same polymers in the fibrous forms (Fig. 5B). Here, the cellular activity is similar on all compositions and the control and there are no statistically significant differences between groups after 7 days of culture. The presence of gelatin in the scaffolds is expected to mediate adhesion via integrin binding, rather than relying on adsorption of serum proteins to the material, which is dependent on the polymer chemistry. After 7 days of culture, MSCs possessed organized actin structures in all groups and appeared to track the direction of the fibers (Fig. 5C). Although these results were only on thin films, future work will investigate cellular population of scaffolds in a three-dimensional context towards tissue development. Importantly, these results indicate that the bulk properties of the scaffolds can be decoupled from cellular adhesion and growth. This feature will expand the potential applications for such scaffolds.

To further increase the diversity of scaffold properties that are attainable, scaffolds were electrospun that contained more than one type of polymer component. This was performed using a recently developed dual-polymer electrospinning apparatus [26], where two spinnerets are targeted to the same rotating mandrel to collect intermixed fibers simultaneously. A new system has also been developed to spin up to three polymer compositions [27]. There were no visible differences in fiber structure or morphology in the dual-polymer scaffolds (Fig. 6A) when compared to single-polymer scaffolds (Fig. 2), indicating that the process does not disrupt fiber formation or mixing. To illustrate fiber mixing, polymers were electrospun with one solution (B6) containing a fluorescent dye. Comparison of the brightfield to fluorescent images clearly shows the mixing of two individual polymer populations (D6 fibers show up in brightfield, but not in fluorescence, whereas B6 fibers

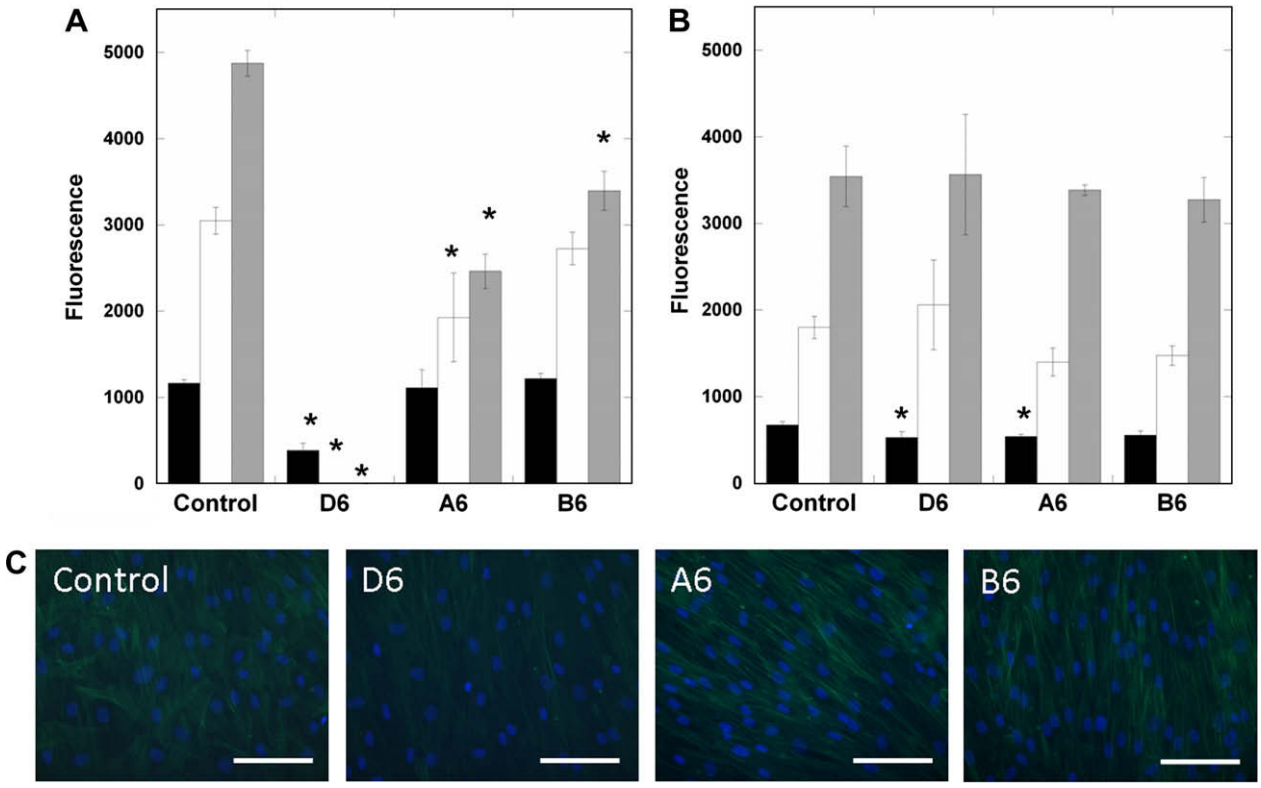

Fig. 5. Cellular interactions with PBAE scaffolds. (A) MSC interactions with films (reported as fluorescence from Alamar blue assay) of D6 (fast), A6 (intermediate) and B6 (slow) polymers after 1 (black), 4 (white) and 7 (grey) days of culture, compared to TCPS controls. (B) MSC interactions with fibrous scaffolds of D6, A6 and B6 polymers for up to 7 days of culture compared to glass controls. (C) Actin and nuclei staining of MSCs on fibrous scaffolds and control glass surfaces after 7 days, illustrating confluence. Scale bar = 100 μm. * $p < 0.05$ vs. control at the respective time point; all groups showed significant differences with culture time, except for the A6 slab formulation between 4 and 7 days.

show up in both) and that distinct polymer populations are retained in the mixture (Fig. 6B).

Importantly, the mixing of fiber populations led to unique mass loss and modulus profiles with time, consisting of features of each fiber population. As mentioned above, the D6 fibers degrade rapidly within a couple of weeks, whereas the B6 fibers exhibit slow mass loss with time. The dual D6/B6 fibers lost mass rapidly during the first 2 weeks, then exhibited little mass loss (Fig. 6C). The initial mass loss is potentially due to the degradation of the D6 fiber population and then mass loss slows when only the B6 fiber population remains. Similar behavior is noted with regard to mechanical properties (Fig. 6D). The modulus of the dual D6/B6 scaffold decreases rapidly, as with the D6 alone scaffolds, but is then maintained with time, as observed with the B6 alone scaffolds. These results clearly illustrate that multi-polymer scaffolds can be designed with features of each type of fiber component. Again, due to the wide variations in potential fiber populations from the combinatorial library, this provides a significant platform with which to design fibrous scaffolds in the future.

Multi-polymer scaffolds have utility in a number of applications. For instance, the dynamic properties that are attained in these systems may be used to maintain uniform properties with time as cells deposit their own matrix in the scaffolding. Also, one problem that has plagued the use of electrospun scaffolds in tissue engineering is the limited cellular infiltration that occurs due to dense packing of fibers, particularly with aligned scaffolds. Several attempts have been made to overcome this by electrospinning fibers of different size scales [33], including poragens during the spinning process [34], or even directly depositing cells into the scaffolds during processing [35]. These approaches have helped advance the field, but are still limited in that they can lead to unstable scaffolds (e.g. delamination). We recently showed that electrospinning a sacrificial fiber population into scaffolds that dissolves away when the scaffold is placed in an aqueous environment could help increase cellular infiltration [26]. This new group of polymers would allow the design of scaffolds where this quickly degrading fiber population could be maintained as long as desired, rather than dissolving immediately.

The importance of these findings lies not in the specific properties that were obtained in this study, particularly since many polymers have been previously electrospun, but in the methodology of using macromers from a combinatorial library to produce diversity in electrospun scaffolds. As the interest in electrospinning and the use of these scaffolds for regenerative medicine increases, so does the need for designing the scaffolds with specific and tunable properties. With this in mind, the main advantages to using a combinatorial library for polymer development are the ease of synthesis (including no purification necessary) and the wide range of properties that are obtained without iterative trial and error procedures. Additionally, these properties can be decoupled from each other, which is difficult to accomplish with distinct iterative polymer development. With the introduction of multi-polymer fabrication, the initial and temporal properties, such as porosity and mechanics, of these scaffolds are endless. Thus, this library can now be a resource to obtain desirable scaffold properties, since this current work indicates that the diversity is retained in the scaffold form. Likewise, this work indicates that cellular interactions may be decoupled from properties such as hydrophobicity and degradation, further expanding their potential.

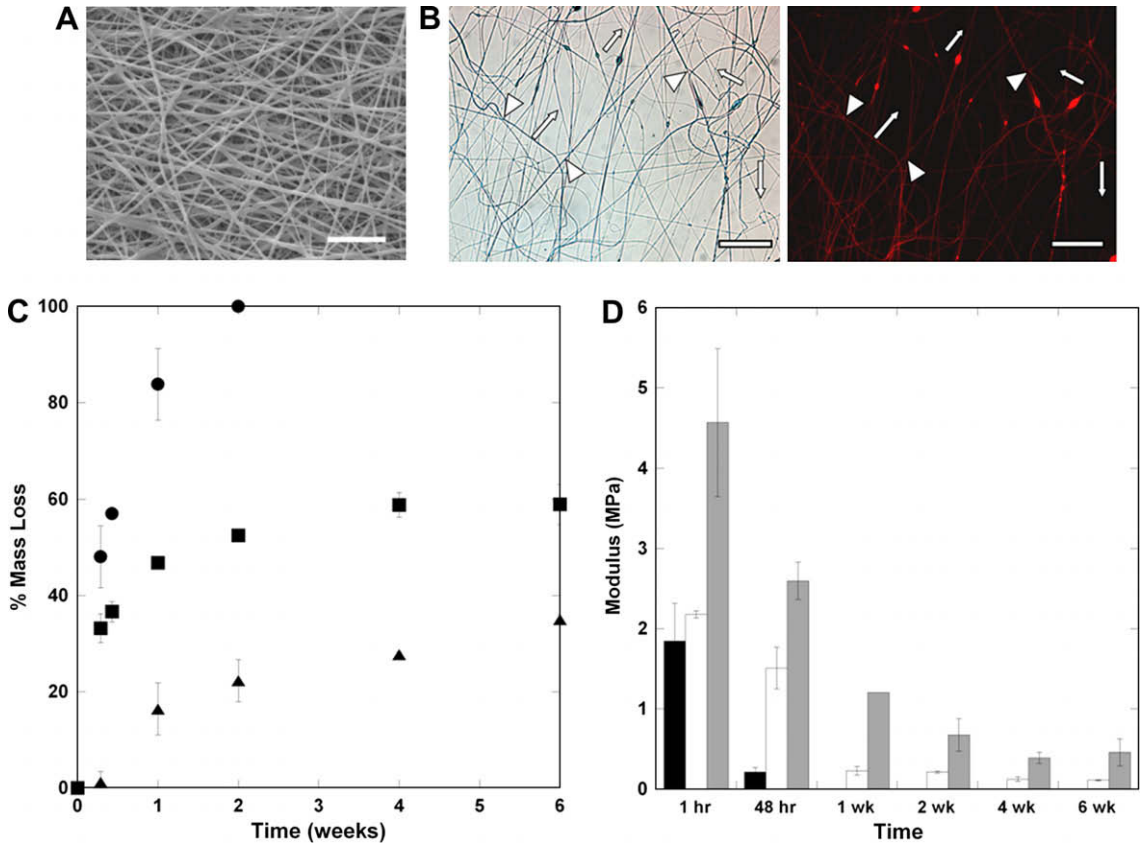

Fig. 6. Multi-polymer scaffolds. (A) SEM of multi-polymer D6/B6 scaffolds (scale bar = 20 μm). (B) Light micrograph and fluorescent image of dual-polymer systems, where a red dye (rhodamine B) was incorporated into the B6 fibers (labeled with triangles) but not into the D6 fibers (labeled with arrows), illustrating the mixing and distribution of distinct fiber populations (scale bar = 50 μm). Mass loss (C) and tensile modulus with degradation (D) profiles of uniform D6 (circles, black bars), uniform B6 (triangles, grey bars) or multi-polymer D6/B6 (squares, white bars) scaffolds.

4. Conclusions

Candidates from a library of biodegradable and reactive macromers that form diverse polymer networks were formed into fibrous scaffolds using electrospinning and exhibited similar variations. Both the mass loss profiles and the mechanical properties (initially and with degradation) followed trends that were observed in bulk polymers. These properties could be correlated to chemical influences, such as hydrophobicity in the original macromers. Adult stem cells adhered and spread on scaffolds from all polymer formulations similarly and there were no differences with controls. A dual-polymer electrospinning process was used to electrospin scaffolds with distinct fiber populations and bulk properties fell between levels of uniform scaffolds for each polymer alone. This technology opens up the possibility of many potential properties in fibrous scaffolds that may be useful in tissue engineering applications.

Acknowledgements

The authors acknowledge assistance from Darren Brey for macromer synthesis and characterization and Brendon Baker for the dual-polymer electrospinning design, Dr. Doug Yates and Dr. Lolita Rotkina for assistance with SEM, and funding from the NIH (R01 AR056624) and the Penn Center for Musculoskeletal Disorders.

Appendix: Figures with essential colour discrimination

Certain figures in this article, particularly Figures 5 and 6, are difficult to interpret in black and white. The full colour images can be found in the on-line version, at doi:10.1016/j.actbio.2009.10.027

References

[1] Mauck RL, Baker BM, Nerurkar NL, Burdick JA, Li WJ, Tuan RS, et al. Engineering on the straight and narrow: the mechanics of nanofibrous assemblies for fiber-reinforced tissue regeneration. Tissue Eng B Rev 2009;15:171–93.
[2] Lu P, Ding B. Applications of electrospun fibers. Recent Pat Nanotechnol 2008;2:169–82.
[3] Nisbet DR, Forsythe JS, Shen W, Finkelstein DI, Horne MK. Review paper: a review of the cellular response on electrospun nanofibers for tissue engineering. J Biomater Appl 2009;24:7–29.
[4] Sill TJ, von Recum HA. Electrospinning: applications in drug delivery and tissue engineering. Biomaterials 2008;29:1989–2006.
[5] Burdick JA, Vunjak-Novakovic G. Review: engineered microenvironments for controlled stem cell differentiation. Tissue Eng A 2009;15:205–19.
[6] Khil MS, Cha DI, Kim HY, Kim IS, Bhattarai N. Electrospun nanofibrous polyurethane membrane as wound dressing. J Biomed Mater Res B Appl Biomater 2003;67:675–9.
[7] Riboldi SA, Sampaolesi M, Neuenschwander P, Cossu G, Mantero S. Electrospun degradable polyesterurethane membranes: potential scaffolds for skeletal muscle tissue engineering. Biomaterials 2005;26:4606–15.
[8] Li WJ, Cooper JA, Mauck RL, Tuan RS. Fabrication and characterization of six electrospun poly(alpha-hydroxy ester)-based fibrous scaffolds for tissue engineering applications. Acta Biomater 2006;2:377–85.
[9] Geng X, Kwon OH, Jang J. Electrospinning of chitosan dissolved in concentrated acetic acid solution. Biomaterials 2005;26:5427–32.
[10] Rho KS, Jeong L, Lee G, Seo BM, Park YJ, Hong SD, et al. Electrospinning of collagen nanofibers: effects on the behavior of normal human keratinocytes and early-stage wound healing. Biomaterials 2006;27:1452–61.
[11] Woerdeman DL, Ye P, Shenoy S, Parnas RS, Wnek GE, Trofimova O. Electrospun fibers from wheat protein: investigation of the interplay between molecular structure and the fluid dynamics of the electrospinning process. Biomacromolecules 2005;6:707–12.
[12] Ji Y, Ghosh K, Shu XZ, Li BQ, Sokolov JC, Prestwich GD. Electrospun three-dimensional hyaluronic acid nanofibrous scaffolds. Biomaterials 2006;27:3782–92.

[13] Brocchini S, James K, Tangpasuthadol V, Kohn J. A combinatorial approach for polymer design. J Am Chem Soc 1997;119:4553–4.
[14] Hoogenboom R, Meier MAR, Schubert US. Combinatorial methods, automated synthesis and high-throughput screening in polymer research: past and present. Macromol Rapid Commun 2003;24:16–32.
[15] Peters A, Brey DM, Burdick JA. High-throughput and combinatorial technologies for tissue engineering applications. Tissue Eng B Rev 2009;15:225–39.
[16] Gordon EM, Barrett RW, Dower WJ, Fodor SPA, Gallop MA. Applications of combinatorial technologies to drug discovery. 2. Combinatorial organic-synthesis, library screening strategies, and future-directions. J Med Chem 1994;37:1385–401.
[17] Brocchini S, James K, Tangpasuthadol V, Kohn J. Structure–property correlations in a combinatorial library of degradable biomaterials. J Biomed Mater Res 1998;42:66–75.
[18] Smith JR, Seyda A, Weber N, Knight D, Abramson S, Kohn J. Integration of combinatorial synthesis, rapid screening, and computational modeling in biomaterials development. Macromol Rapid Commun 2004;25:127–40.
[19] Anderson DG, Tweedie CA, Hossain N, Navarro SM, Brey DM, Van Vliet KJ, et al. A combinatorial library of photocrosslinkable and degradable materials. Adv Mater 2006;18:2614–8.
[20] Akinc A, Lynn DM, Anderson DG, Langer R. Parallel synthesis and biophysical characterization of a degradable polymer library for gene delivery. J Am Chem Soc 2003;125:5316–23.
[21] Lynn DM, Anderson DG, Putnam D, Langer R. Accelerated discovery of synthetic transfection vectors: parallel synthesis and screening of degradable polymer library. J Am Chem Soc 2001;123:8155–6.
[22] Anderson DG, Tweedie CA, Hossain N, Navarro SM, Brey DM, Van Vliet KJ, et al. A combinatorial library of photocrosslinkable and degradable materials. Adv Mater 2006;18:2614–8.
[23] Brey DM, Erickson I, Burdick JA. Influence of macromer molecular weight and chemistry on poly(beta-amino ester) network properties and initial cell interactions. J Biomed Mater Res A 2008;85A:731–41.
[24] Brey DM, Ifkovits JL, Mozia RI, Katz JS, Burdick JA. Controlling poly(beta-amino ester) network properties through macromer branching. Acta Biomater 2008;4:207–17.
[25] Tan AR, Ifkovits JL, Baker BM, Brey DM, Mauck RL, Burdick JA. Electrospinning of photocrosslinked and degradable fibrous scaffolds. J Biomed Mater Res A 2008;87:1034–43.
[26] Baker BM, Gee AO, Metter RB, Nathan AS, Marklein RA, Burdick JA. The potential to improve cell infiltration in composite fiber-aligned electrospun scaffolds by the selective removal of sacrificial fibers. Biomaterials 2008;29:2348–58.
[27] Baker BM, Nerurkar NL, Burdick JA, Elliott DM, Mauck RL. Fabrication and modeling of dynamic multipolymer nanofibrous scaffolds. J Biomech Eng 2009;131:101012.
[28] Baker BM, Mauck RL. Nanofiber alignment enhances the development of engineered meniscus constructs. Tissue Eng 2007;28:1967–77.
[29] Ifkovits JL, Padera RF, Burdick JA. Biodegradable and radically polymerized elastomers with enhanced processing capabilities. Biomed Mater 2008;3:034104.
[30] Li M, Guo Y, Wei Y, MacDiarmid AG, Lelkes PI. Electrospinning polyaniline-contained gelatin nanofibers for tissue engineering applications. Biomaterials 2006;27:2705–15.
[31] Allen LT, Tosetto M, Miller IS, O'Connor DP, Penney SC, Lynch I, et al. Surface-induced changes in protein adsorption and implications for cellular phenotypic responses to surface interaction. Biomaterials 2006;27:3096–108.
[32] Wang YX, Robertson JL, Spillman Jr WB, Claus RO. Effects of the chemical structure and the surface properties of polymeric biomaterials on their biocompatibility. Pharm Res 2004;21:1362–73.
[33] Pham QP, Sharma U, Mikos AG. Electrospun poly(epsilon-caprolactone) microfiber and multilayer nanofiber/microfiber scaffolds: characterization of scaffolds and measurement of cellular infiltration. Biomacromolecules 2006;7:2796–805.
[34] Nam J, Huang Y, Agarwal S, Lannutti J. Improved cellular infiltration in electrospun fiber via engineered porosity. Tissue Eng 2007;13:2249–57.
[35] Stankus JJ, Guan J, Fujimoto K, Wagner WR. Microintegrating smooth muscle cells into a biodegradable, elastomeric fiber matrix. Biomaterials 2006;27:735–44.